

TiO₂-Assisted Photodegradation of Dyes. 9. Photooxidation of a Squarylium Cyanine Dye in Aqueous Dispersions under Visible Light Irradiation

TAIXING WU,[†] TONG LIN,[†]
JINCAI ZHAO,^{*,†} HISAO HIDAKA,[‡] AND
NICK SERPONE[§]

Institute of Photographic Chemistry, Chinese Academy of Sciences, Beijing 100101, China, and Department of Chemistry, Meisei University, 2-1-1 Hodokubo, Hino, Tokyo 191, Japan, and Department of Chemistry & Biochemistry, Concordia University, Montreal, Canada H3G 1M8

The TiO₂-assisted photodegradation of a squarylium cyanine dye (SQ) has been examined under visible light irradiation ($\lambda \geq 430$ nm) by UV-vis, proton-NMR, ESR, and GC-MS spectroscopies, by peroxide assays in the presence of peroxidase and catalase enzymes, and by chemical oxygen demand (COD) methods. Significant results were obtained relevant to the mechanism(s) of TiO₂-assisted photodegradations. The active oxygen species produced first when an aqueous TiO₂ dispersion containing SQ is irradiated by visible light is the superoxide radical anion, which is stable in methanol solvent but very unstable in aqueous media, and is readily converted to $\cdot\text{OH}$ radicals via formation and subsequent reduction of H₂O₂. The quantity of H₂O₂ increased during the photodegradation; though expected, no organoperoxides were detected. Of import, cleavage of the cyanine C=C double bond in the SQ dye dominated over the whole degradation process yielding 1-sulfopropyl-3,3-dimethyl-5-bromindolenium-2-one, the predominant component in the dispersion. This intermediate is not excited by visible light and degrades no further. A sequence of steps is proposed in the initiation of the TiO₂-assisted photochemical transformation.

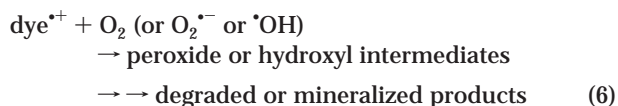
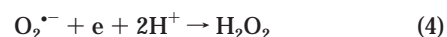
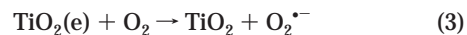
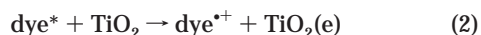
Introduction

Much attention has been directed at investigating the photocatalytic degradation of organic pollutants mediated by TiO₂ particles in aqueous dispersions under UV-light irradiation. The body of data suggests a possible and effective approach toward the degradation or mineralization of a wide variety of harmful/toxic organic pollutants in wastewaters and toward the purification of drinking water.^{1–6} However, solar UV-light reaching the surface of the earth and available to excite TiO₂ is relatively small (ca. 3–5% of the AM1 solar spectrum), and artificial UV light sources are somewhat expensive. Therefore, recent efforts have been focused at exploring means to utilize effectively the cheaper visible light

sources or to use a greater quantity of the inexhaustible visible sunlight for treating polluted ecosystems.

Dyestuffs represent a class of organic pollutants that absorb visible light. Electron transfer processes occurring between dyes and semiconductors, especially TiO₂, have been examined and found to have practical potential.^{7–9} Kamat and co-workers¹⁰ reported the photodegradation of Acid Orange 7 and Naphthol Blue Black dyes preadsorbed on the surface of TiO₂ particles, and Ross et al.¹¹ examined the degradation of terbutylazine under visible irradiation on TiO₂ particles sensitized by rose bengal, in which the photodecomposition of the sensitizer was also TiO₂-assisted.

We recently reported the photodegradation of several dyes under exposure to visible light in the presence of TiO₂ nanoparticulates.^{12–14} The visible-irradiation mechanism (eqs 1–6) is clearly different from the UV-irradiation pathway described previously;^{14a} the dye not the semiconductor TiO₂ is excited by visible light:



The excited dye injects an electron to the conduction band of TiO₂, whence it is scavenged by preadsorbed oxygen, O₂, to form active oxygen radicals similar to those in UV-irradiation processes. These active radicals drive the photodegradation or mineralization. TiO₂ plays the significant role of an electron carrier leading to separation of injected electrons and cationic dye radicals. Such assisted photoprocesses provide an attractive route to treat or pretreat dye pollutants using artificial visible light or sunlight. More extensive and detailed investigations are necessary to gain a further understanding of these processes.

In the present study, the laser dye squarylium cyanine (SQ) was chosen as the substrate whose visible light driven photodegradation in aqueous TiO₂ dispersions was monitored by chemical oxygen demand (COD_{Cr}) measurements and by UV-vis, proton-NMR, GC-MS, and DMPO spin trap electron spin resonance (ESR) spectroscopies. To gain further insights on the initial steps of the photoprocesses, we also examined the transformation of the SQ dye in the presence of the superoxide dismutase (SOD) and catalase (Cat) enzymes. The active oxygen species produced first was the superoxide radical anion under the experimental conditions used. This species is stable in methanol solvent but very unstable in aqueous solution, ultimately converted to $\cdot\text{OH}$ radicals via formation and subsequent reduction of H₂O₂.

Experimental Section

Materials. TiO₂ nanoparticulates (P25, ca. 80% anatase, 20% rutile; BET area, ca. 50 m² g⁻¹) were kindly supplied by Degussa Co. The spin trap 5,5-dimethyl-1-pyrroline-*N*-oxide (DMPO) was purchased from Sigma Chemical Co. The squarylium cyanine dye (see structure below; letters identify the protons for NMR purpose) was synthesized according to

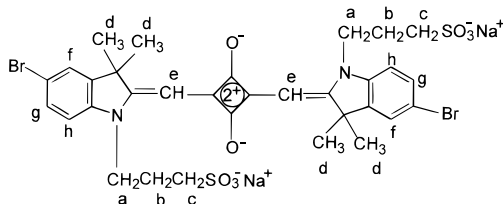
* Corresponding author fax: +86-10-6487-9375; e-mail: jczhao@ipc.ac.cn.

[†] Chinese Academy of Sciences.

[‡] Meisei University.

[§] Concordia University.

the method of Lin and Peng.¹⁵ Horseradish peroxidase (POD) was purchased from Huamei Biologic Engineering Co. (China), the superoxide dismutase (SOD) was obtained from the Research & Development Center of Biochemicals Co. (Hebei, China), and the *N,N*-diethyl-*p*-phenylenediamine



(DPD) reagent from Merck (p.a.). Other chemicals were all of analytical reagent grade quality and used without further purification. Fe^{3+} was from FeCl_3 . Deionized and doubly distilled water was used throughout this study. The pH of aqueous solutions was adjusted by diluted NaOH or HClO_4 aqueous solutions, as needed.

Photoreactor and Light Source. A 500-W halogen lamp (Institute of Electric Light Source, Beijing) was positioned inside a cylindrical Pyrex vessel surrounded by a circulating water jacket (Pyrex) to cool the lamp. A cutoff filter was also placed outside the Pyrex jacket to remove radiation below 420 nm completely and to ensure irradiation of the dispersion only by visible light wavelengths.

Procedures and Analyses. Aqueous TiO_2 suspensions were prepared by adding 4 mg of TiO_2 powder to a 50 mL of aqueous dye solution [$\text{SQ}] = 8.26 \times 10^{-6} \text{ M}$]. Prior to irradiation the suspensions were magnetically stirred in the dark for ca. 30 min to ensure establishment of an adsorption/desorption equilibrium of dye under air-atmosphere (equilibrated $[\text{O}_2]$ achieve up to $2.4 \times 10^{-4} \text{ M}$ in aqueous dispersions, enough for dye degradation). At given irradiation time intervals, 3-mL aliquots were collected, centrifuged, and then filtered through a Millipore filter (pore size $0.22 \mu\text{m}$) to remove the TiO_2 particulates. The filtrates were analyzed by recording variations in the UV-vis spectra of the SQ dye with a Shimadzu-160A spectrophotometer. Chemical oxygen demand (COD_{Cr}) was assayed by the potassium dichromate titration method¹⁶ obtained by directly measuring the COD_{Cr} of $8.26 \times 10^{-5} \text{ M}$ SQ suspensions (45 mL) containing 25 mg of the TiO_2 particulates.

The concentration of total peroxides (including organoperoxides and H_2O_2) formed during irradiation of a 50-mL solution of SQ ($8.26 \times 10^{-5} \text{ M}$) containing 25 mg of TiO_2 was detected immediately after removal of TiO_2 particles by centrifugation and filtration and after irradiation at various time intervals by the DPD method, a photometric method ($\lambda = 551 \text{ nm}$, $\epsilon = 21\,000 \text{ M}^{-1} \text{ cm}^{-1}$ per peroxide) in which the DPD reagent is oxidized by H_2O_2 and/or by the organoperoxide based on the peroxidase catalyzed reaction.¹⁷ Electron paramagnetic resonance (ESR) signals of paramagnetic species spin-trapped with DMPO were recorded with a Bruker EPR 300E spectrometer to measure formation of active radical species during irradiation of the dye dispersion ($8.26 \times 10^{-5} \text{ M}$) containing 25 mg of TiO_2 particles; in this case, the irradiation source ($\lambda = 532 \text{ nm}$) was a Quanta-Ray Nd:YAG pulsed (10 pulses per second) laser system. The settings for the ESR spectrometer were center field = 3486.70 G; sweep width = 100.0 G; microwave frequency = 9.82 GHz; and power = 5.05 mW. The volume of the dispersions was 0.4 mL; DMPO, 0.22 M, 50 μL ; pH = 3.8.

Proton NMR spectra were obtained with a Varian 300 nuclear magnetic resonance spectrometer. Samples for ^1H NMR spectra were prepared as follows: several dispersions

containing 20 mL of the SQ dye ($8.26 \times 10^{-4} \text{ M}$) and 50 mg of TiO_2 were irradiated at different time intervals; the TiO_2 particles were removed by centrifugation and filtration as described above. Subsequently, the solvent of the filtrate was removed (below 50°C) under reduced pressure. The remaining residue was dissolved in 0.5 mL DMSO- d_6 for NMR determination.

The sample for the gas chromatography/mass spectroscopy (Trio-2000, equipped with a BPX70 column, size $28 \text{ m} \times 0.25 \text{ mm}$) experiments was prepared in a manner otherwise identical to that for ^1H NMR; however, the final residue was dissolved in methanol. Ion chromatography (Shimadzu LC-10AS) was used to determine the quantity of Br^- and SO_4^{2-} ions derived from the sulfonate group in the SQ dye during the photodegradation of an $8.26 \times 10^{-5} \text{ M}$ SQ solution.

Results and Discussion

UV-vis Spectral Changes. The squarylium cyanine dye SQ is highly soluble in water and is strongly adsorbed on the TiO_2 particle surface through the two sulfonate groups (see structure above). In fact, the dye molecules are adsorbed completely on the TiO_2 particles on addition of 20 mg of TiO_2 to a 50 mL aqueous solution of SQ ($8.26 \times 10^{-6} \text{ M}$). To assess more precisely adsorption and degradation of SQ in the presence of TiO_2 under visible light irradiation, 4 mg of TiO_2 was added to 50 mL of the $8.26 \times 10^{-6} \text{ M}$ SQ solution (much less than the quantity of TiO_2 , 100 mg, used in the photodegradation of Rhodamine B reported earlier^{14a}). As illustrated in Figure 1, adsorption of the SQ cyanine dye on the TiO_2 surface is about 23% under the conditions used (see Figure 1 caption). Under irradiation, the characteristic absorption band at ca. 630 nm decreases rapidly, whereas the 257-nm band increases with increasing irradiation time; concomitantly, the color of the dispersion changed from initial black-blue color to green to a very light yellow, indicating that at least the chromophoric structure of the squarylium cyanine dye was destroyed.

The inset in Figure 1 shows the temporal concentration changes of SQ under the same conditions as in Figure 2 (see below) illustrating zero order kinetics at least for the first 8 min of irradiation; $k = 5.38 \times 10^{-7} \text{ M}^{-1} \text{ min}^{-1}$. The fact that rapid decomposition occurs is consistent with the notion that relatively strong adsorption enhances photodegradation on the TiO_2 surface.^{12b,13b,14b} Control experiments show that the SQ dye does not degrade in TiO_2 suspensions in the dark or under visible light in the absence of the TiO_2 particulates, under otherwise identical experimental conditions.

After ca. 20 min of illumination, only the 257-nm band remains which coincides exactly with the absorption spectrum of the 1-sulfopropyl-5-bromo-2,3,3-trimethylindolenium species. New features, albeit of weak intensity, appeared in the wavelength range 350–450 nm. To scrutinize the temporal changes of these new features, the SQ concentration was increased by an order of magnitude to $8.26 \times 10^{-5} \text{ M}$ to amplify the spectral changes; they are displayed in Figure 2a,b.

After the first 16 min of irradiation, a new band appears at ca. 430 nm whose intensity increases with time. Subsequently, this new band diminishes during the next 16 min irradiation period (Figure 2b) to disappear completely after ~ 70 min of illumination with evolution of yet another band around 350 nm. Also evidenced by the results from the proton NMR and GC-MS experiments (see below), the above events implicate the occurrence of a two-step decomposition process: the first is detachment of one indolenium moiety from the SQ dye structure leaving a larger fragment consisting of the indolenium fragment and the squaraine acid moiety which has an absorption at ca. 430 nm with intensity smaller

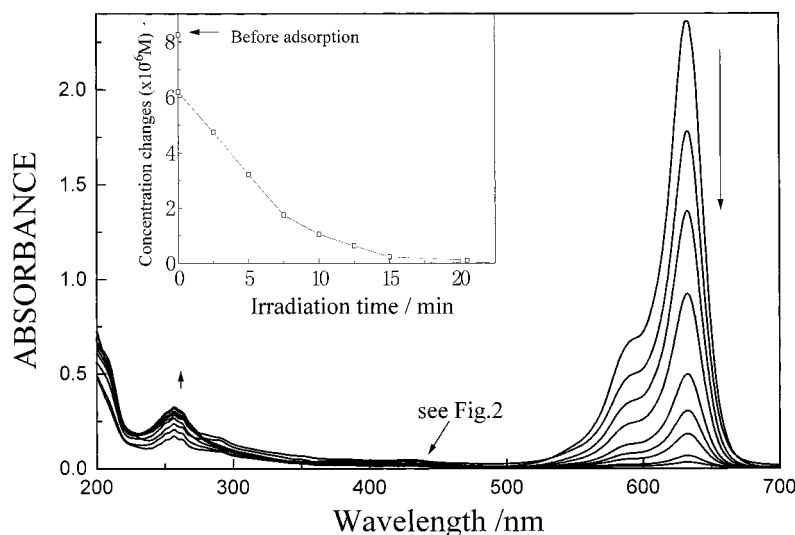


FIGURE 1. UV-vis spectral changes of the squarylium cyanine dye SQ (8.26×10^{-6} M, 50 mL) in aqueous TiO_2 dispersions with irradiation time. Spectra from top to bottom refer to before addition of TiO_2 particles; equilibrium concentration after addition of TiO_2 particles (3 mg/50 mL); irradiation for 2.5, 5.0, 7.5, 10.0, 12.5, and 20.5 min, respectively. Inset: SQ concentration changes with irradiation time under the same conditions.

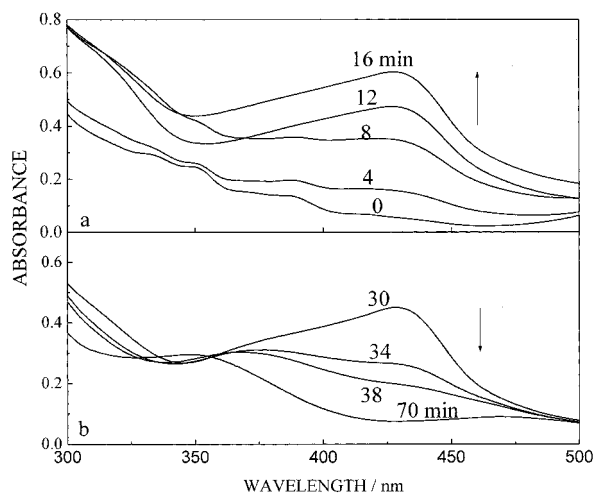


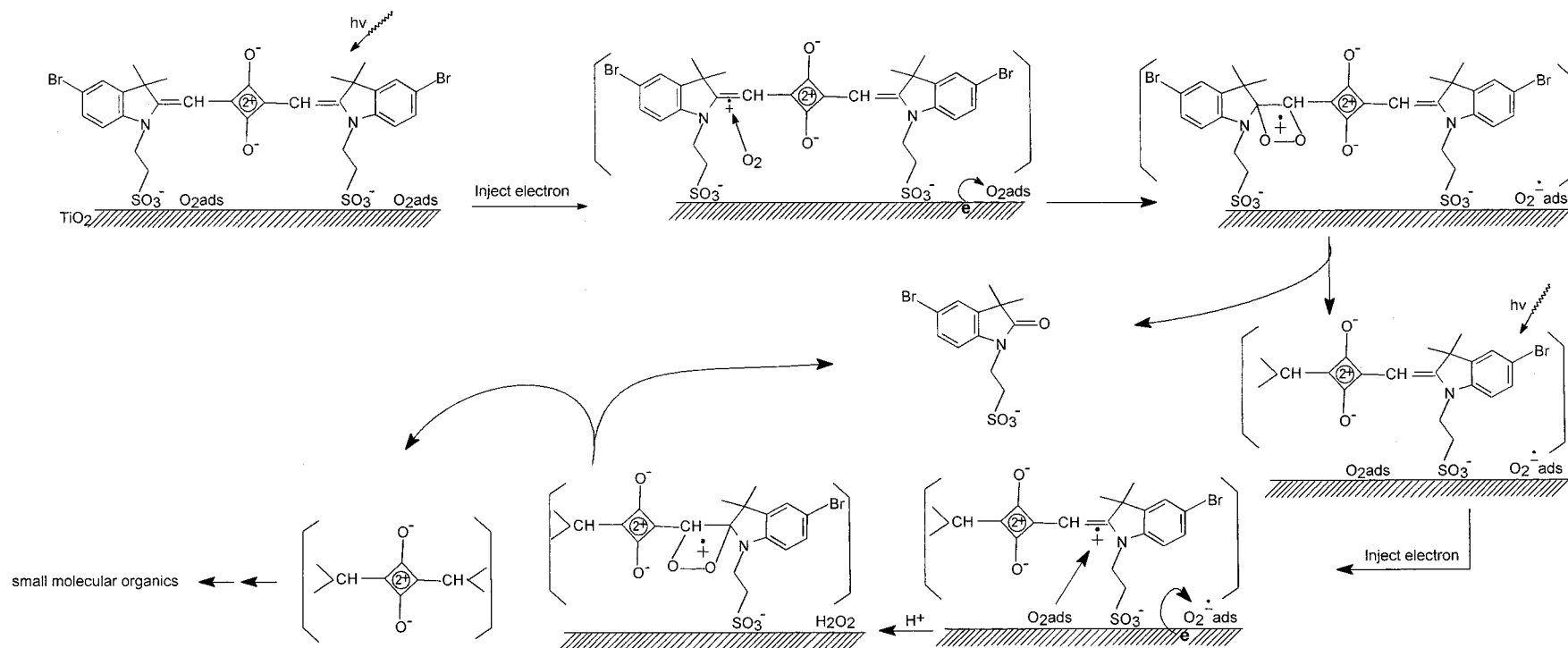
FIGURE 2. UV-vis spectral changes of SQ in the range 300–500 nm with irradiation time under the same conditions as those of Figure 1 except that the initial [SQ] was 8.26×10^{-5} M and TiO_2 , 30 mg.

than of the 630-nm band of the original structure of the SQ dye; the second is decomposition of the larger fragment into another indolenium moiety and the squaraine acid moiety or its fragments (see Scheme 1). In the solution bulk and on the TiO_2 surface, a fast dynamic equilibrium exists between the SQ dye and the cleaved indolenium fragment and the squaraine acid group, albeit the SQ dye or degraded fragments are strongly adsorbed to the TiO_2 surface through the sulfonate groups as witnessed by the UV-vis spectral features at 430 nm for the fragments in the bulk solution (Figure 2a,b).

COD Assays. Chemical oxygen demand (COD) values reflect the degree to which the degradation or mineralization of an organic species has occurred, whereas production of inorganic species such as bromide and sulfate ions indicates the conversion of the heteroatoms in the SQ dye. COD measurements were done on several 45-mL samples of an 8.26×10^{-5} M SQ aqueous solution at given time intervals in the presence of TiO_2 particles (25 mg) under visible light irradiation (concentration changes of SQ are shown as the curve "SQ" in Figure 5 below). Only small COD changes ($\sim 12\%$) are evident within the first 40 min, after which the

COD value no longer changes on further irradiation (Table 1). Concomitantly, ion chromatography was employed to examine whether inorganic ions were produced under the same experimental conditions. Neither bromide nor sulfate ions were detected. These two significant results support the notion that simple dissociation of SQ molecules takes place (small COD changes) and that the end fragment thus produced cannot be degraded further to give inorganic bromide and/or sulfate ion. We attribute this to the lack of absorption of visible light by the fragment(s).

^1H NMR and GC-MS Spectra. To clarify the nature of the main degraded intermediates and the degradation process, time-resolved ^1H NMR profiles were obtained for several 20 mL samples of 8.26×10^{-4} M SQ aqueous TiO_2 dispersions illuminated individually under the same conditions for different time intervals (Figure 3). Prior to photodegradation, the NMR spectrum of the SQ dye revealed (spectrum a) chemical shifts of the aromatic hydrogens H_f , H_i , and H_g at 7.80, 7.55, and 7.43 ppm, respectively, whereas the protons H_e on the $\text{C}=\text{C}$ double bond are seen at 5.83 ppm and the methylene hydrogens H_a , H_b , and H_c of the *N*-sulfoethyl group are seen at 4.22 ppm (peak triplet for the methylene nearest the N atom), 2.0 ppm (peak quintuplet for the middle methylene group), and at 2.55 ppm (peak triplet for the methylene near the sulfonic group). The 12 hydrogens (H_d) belonging to the four methyl groups showed a strong single peak at 1.70 ppm. These $-\text{CH}_3$ proton signals shifted to characteristic positions at higher field (1.25 ppm), and their intensity increased gradually with prolonged irradiation time. The signals of the aromatic protons shifted to 7.62, 7.44, and 7.12 ppm, respectively; the methylene hydrogens of the *N*-sulfoethyl group moved to 3.72 ppm (H_a near N atom), 2.45 ppm (H_c near sulfonic group), and 1.83 ppm (H_b , middle methylene). The more significant change is the progressive disappearance of the proton signals (at 5.83 ppm) of the $>\text{C}=\text{CH}-$ function caused by cleavage of the $\text{C}=\text{C}$ bond. After 30 h of irradiation, proton NMR signals no longer varied, indicating the end of the degradation process. These results confirm that the decomposition of the SQ dye in TiO_2 suspensions under visible irradiation begins with cleavage of the $\text{C}=\text{C}$ double bond, and the detached main fragment is 1-sulfoethyl-5-bromo-3,3-dimethylindolenium-2-one. Because the indolenium structure is less conjugated than the original SQ molecule causes the proton signals in the indolenium fragment to occur at higher field.

SCHEME 1. Proposed Pathway for the TiO_2 -Assisted Photodegradation of SQ under Visible Light Irradiation

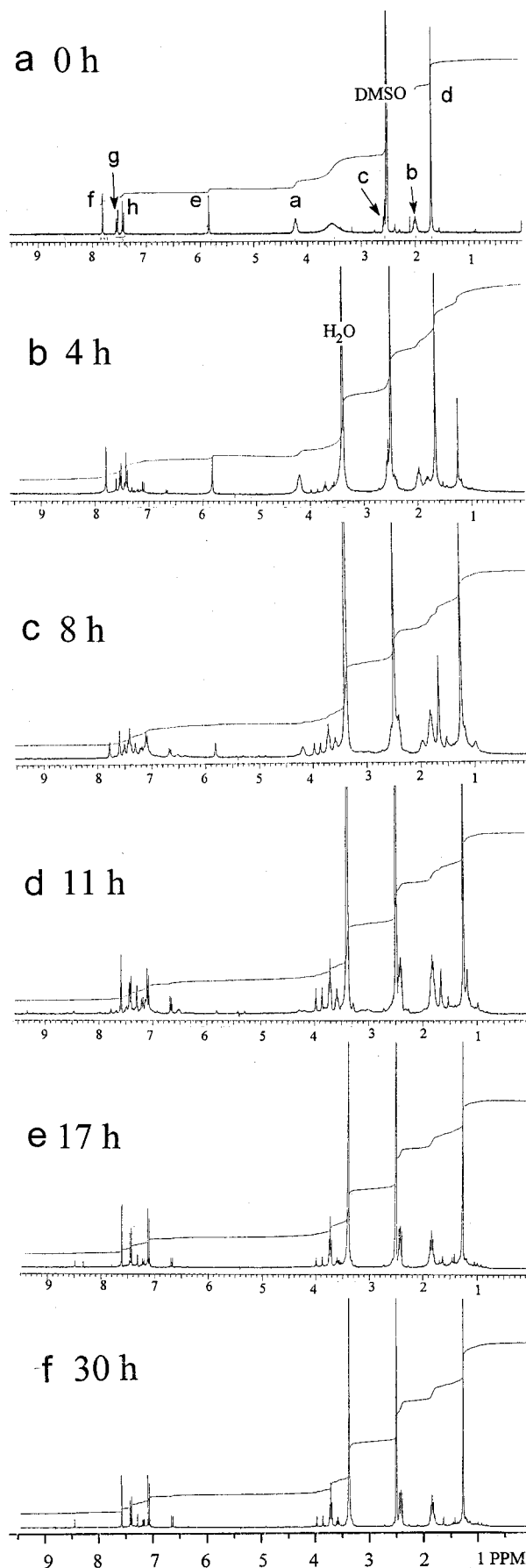


FIGURE 3. Temporal profile of ^1H NMR spectra at various irradiation intervals during the photodegradation of the squarylium cyanine dye SQ.

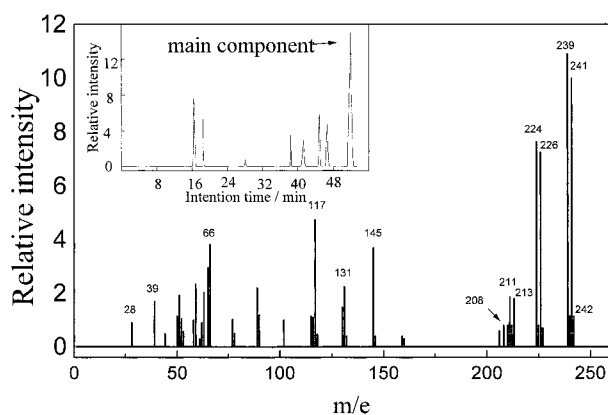


FIGURE 4. Mass spectral data of the major GC component (see inset). See text for details.

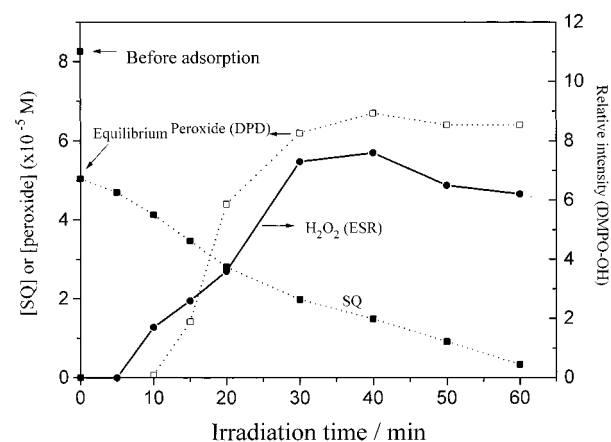


FIGURE 5. Changes of SQ concentration (solid square) and H_2O_2 formed during the photodegradation process. Open squares [peroxide (DPD)] refer to the peroxide concentration measured by the DPD method. Solid circles [H_2O_2 (ESR)] denote the H_2O_2 concentration detected for the DMPO- $\cdot\text{OH}$ adduct with the DMPO spin-trap ESR technique after addition of DMPO and Fe^{3+} ($2 \times 10^{-5} \text{ M}$) to the SQ/ TiO_2 dispersions irradiated for different time intervals by visible light (halogen lamp). Note that the concentration of Fe^{3+} must be controlled so that no extraneous ESR signals appear in blank experiments.^{20,25}

TABLE 1. COD Changes of SQ (45 mL, $8.26 \times 10^{-5} \text{ M}$) with Irradiation Time

irradiation time (min)	0	20	30	40	60
$[\text{COD}_0 - \text{COD}_t] / \text{COD}_0, \%$	0	6	10	12	12

Further supporting evidence was obtained by GC-MS spectroscopy; the results of which are depicted in Figure 4. The predominant peak in the GC chromatogram (see inset to Figure 4) was analyzed in detail by mass spectroscopy. As expected, the main component contains one bromine atom responsible for the appearance of several two mass peaks of nearly equal intensity due to the presence of bromine isotopes. The mass spectral analysis (see Scheme 2) also confirms that the major component is the degraded fragment 1-sulfopropyl-5-bromo-3,3-dimethylindolenium-2-one species. These results also offer the opportunity to use the TiO_2 -assisted method for organic synthetic purposes. The main fragmentation pattern for this GC major component are produced through two principal paths: one implicates homolytic fission of the sulfopropyl- N bond and the second involves a McLafferty rearrangement. The former yields the fragments with $m/e = 239$ and 241 amu and $m/e = 145$ amu which lose $-\text{CH}_3$ and $-\text{CH}_2$ groups to produce smaller cation radical fragments. In the McLafferty rearrangement, the major

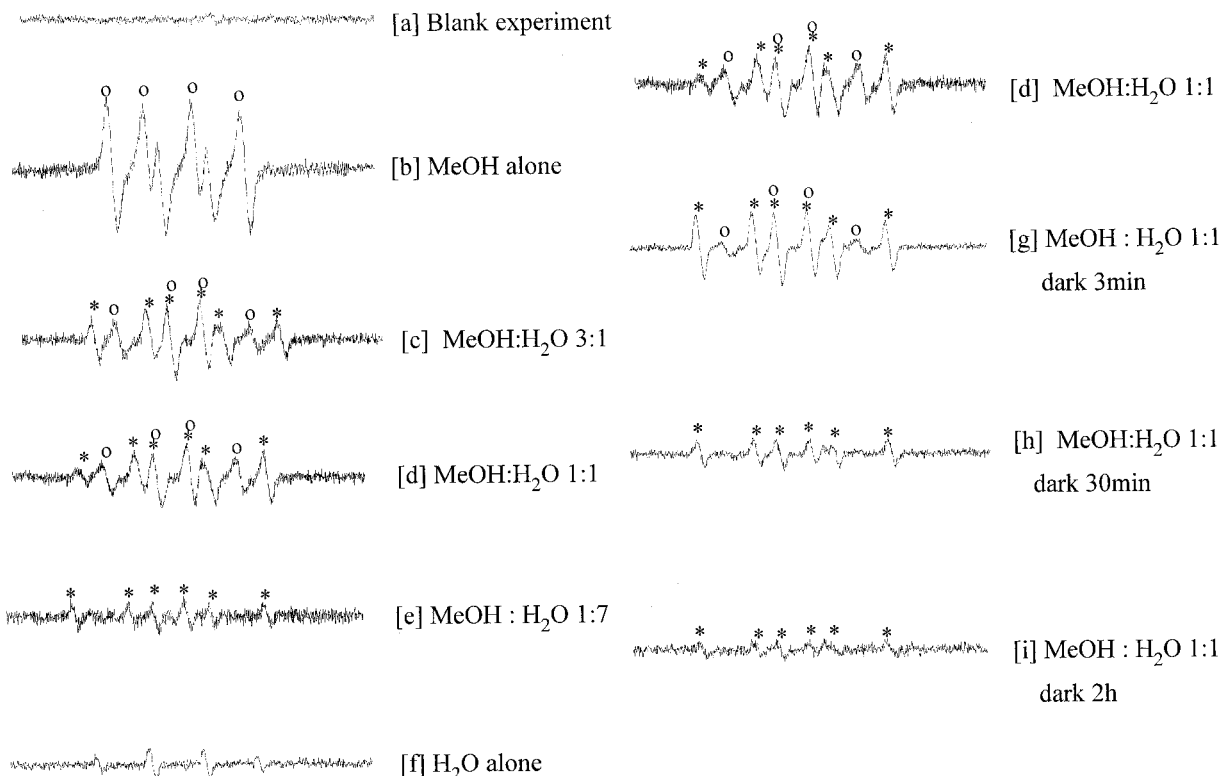
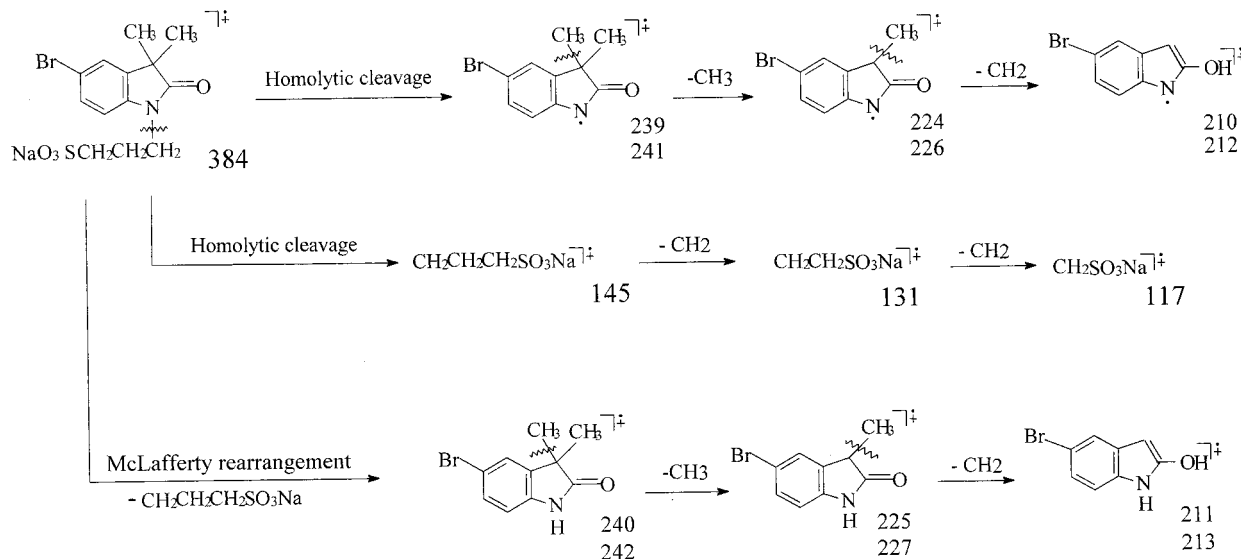


FIGURE 6. DMPO spin-trap ESR spectra of SQ/TiO₂ dispersions at different ratios of CH₃OH to H₂O under laser irradiation at $\lambda = 532$ nm. Irradiation time: 160 s; total volume, 0.4 mL; TiO₂, 4 mg; DMPO, 50 μ L (0.22 M). Spectra (g) to (i) show decay of spectrum (d) at different times in the dark. Open circles placed above certain peak signals refer to ESR signals of the DMPO-OOH adduct, and the asterisks denote signals due to the DMPO-CH₂OH adduct.

SCHEME 2. Fragmentation Pattern of the Major Component in the Breakdown of the SQ Chromophore, Namely the 1-Sulfopropyl-3,3-dimethyl-5-bromoindolenium-2-one Species



GC component ($m/e = 384$ amu) loses the sulfopropyl group to give a fragment with $m/e = 240$ and 242 amu of nearly equal intensity; it subsequently fragments further by loss of $-\text{CH}_3$ and $-\text{CH}_2$ groups. The double m/e values are those inferred above to arise from the presence of the Br isotopes.

Formation of Peroxides. Production of peroxides such as H₂O₂ and organoperoxides, ROOH, is a reasonable expectation (see eqs 1–7); their presence was probed in visible light illuminated aqueous SQ/TiO₂ dispersions using the catalyzed oxidation of the *N,N*-diethyl-*p*-phenylenediamine (DPD) reagent by the POD enzyme. After 40 min irradiation,

the 8.26×10^{-5} M SQ dye solution is totally discolored (bleached) pointing to a break-up of the chromophoric entity. After a 10-min induction period, the peroxide concentration increases from 0 to 6.7×10^{-5} M (open squares, Figure 5) on continued irradiation to 40 min, after which it remains constant with further illumination for an additional 20 min.

The DPD method assays the total quantity of peroxides {H₂O₂ + organoperoxide (ROOH)}.¹⁷ To ascertain whether the peroxide is H₂O₂ and/or an organoperoxide in the total amount formed, DMPO spin-trapping ESR experiments were carried out to probe whether DMPO- $\cdot\text{OH}$ adducts are formed

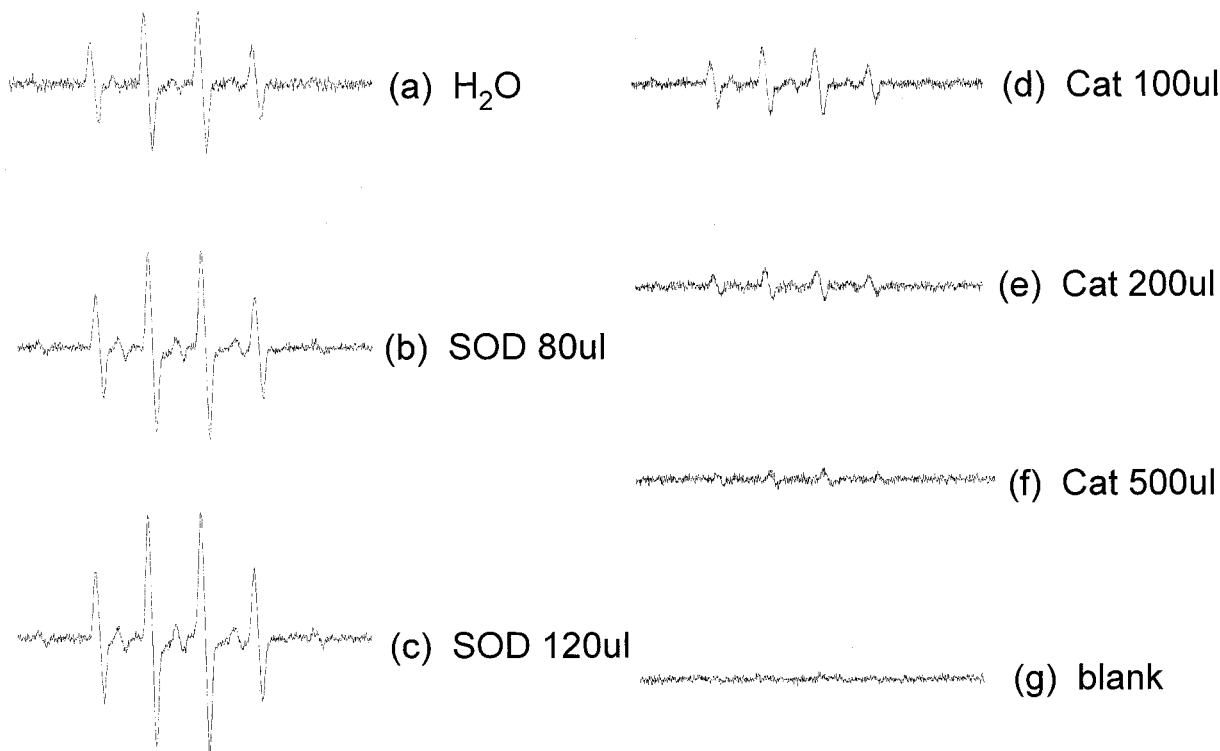
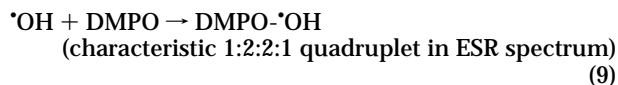
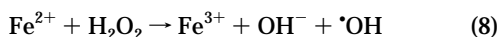
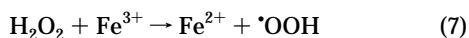
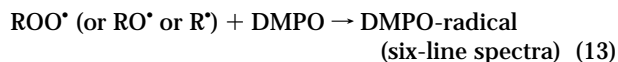
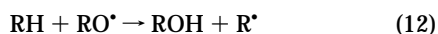
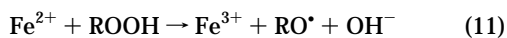
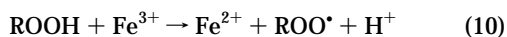


FIGURE 7. Effect of addition of SOD or catalase on the intensity of the DMPO- \cdot OH adduct ESR signal in the SQ/TiO₂ system. Conditions: SOD, 2.5 mg mL⁻¹, activity, 8000 U mg⁻¹; catalase, 2.0 mg mL⁻¹, activity, greater than 2.0 U mg⁻¹; total volume of the tested solution: 0.6 mL; phosphate buffer, 0.2 mL; initial SQ concentration, 8.26×10^{-5} M; TiO₂, 4 mg.

in illuminated dispersions containing the squarylium cyanine dye. Hydroxyl radicals are produced when H₂O₂ reacts with Fe³⁺ (eqs 7 and 8)^{18,19} which in the presence of the spin-trapping reagent DMPO gives DMPO- \cdot OH adducts (eq 8) whose ESR signals with intensity 1:2:2:1 are characteristic of spin-trapped \cdot OH radicals (eq 9):



By contrast, alkoxy (RO \cdot) or alkyl (R \cdot) radicals formed from the reaction of the organoperoxide ROOH with Fe³⁺ species (eqs 10–13) produce DMPO- \cdot OR, DMPO- \cdot OOR, or DMPO- \cdot R adducts with DMPO all of which typically display a six-line ESR spectrum for the oxygen-centered and carbon-centered radical in the aqueous system.^{20,21}



RH represents the organic compound. Accordingly, the aqueous dispersion irradiated for different time intervals by visible light (halogen lamp) was sampled, and then DMPO and Fe³⁺ were added to probe the organoperoxy radicals by the spin-trap ESR technique.

ESR experiments reveal only signals of the DMPO- \cdot OH radical adduct whose characteristic signals increase in intensity with irradiation time, showing a tendency similar

to the peroxide concentration determined by the DPD method (solid circles, Figure 5). The six-line ESR spectra expected for the O- or C-centered radical adduct did not materialize, thereby indicating that only H₂O₂ forms on irradiation.

Further evidence was sought to clarify which of the peroxide forms in the illuminated suspensions by addition of the catalase enzyme to discriminate between hydrogen peroxide and the organoperoxides. Catalase can decompose hydrogen peroxide to H₂O and O₂^{22,23} but hardly affects organoperoxides, especially long-chain organoperoxides.²³ Thus, catalase was added to remove H₂O₂ formed in the degraded solution (3 mL of sample was taken) after irradiation, and the presence of organoperoxides was subsequently assayed by the DPD method. The results show that the two peaks at 510 nm and 550 nm produced by DPD reagent oxidation were not observed, inferring that no organoperoxides formed after irradiating the SQ/TiO₂ dispersion for 30 min (and for 60 min).

These observations demonstrate that the peroxide formed during the photodegradation process is primarily H₂O₂, although we cannot preclude the possibility that if any ROOH did form it might decompose too rapidly leaving an undetectable steady-state concentration of the organoperoxide.

ESR Spectra. ESR spectra of DMPO spin adducts were recorded following irradiation of SQ/TiO₂ suspensions with pulsed laser illumination at $\lambda = 532$ nm. A spectrum displaying signals with characteristic intensity 1:2:2:1 for DMPO- \cdot OH adducts was obtained showing that the \cdot OH radical was indeed formed under the prevailing conditions. However, eqs 3–5 suggest that the first radical formed and then spin-trapped should be the superoxide radical anion (or the hydrosuperoxide radical in acid media). To delineate the events, we carried out sequential ESR experiments in which the CH₃OH to H₂O ratio in the mixed solvent system was varied to ascertain the generation of the superoxide radical anion. As illustrated in spectrum (b) of Figure 6, strong

DMPO- $\cdot\text{OOH}$ or DMPO- $\text{O}_2^{\cdot-}$ adduct signals are evident in methanol solvent alone on irradiating a methanolic SQ/TiO₂ dispersion, whereas DMPO- $\cdot\text{OH}$ adduct signals are evident only in irradiated aqueous TiO₂ dispersions {spectrum (f) of Figure 6}. Moreover, addition of smaller quantities of H₂O to methanolic dispersions containing TiO₂ and SQ resulted in composite ESR spectra that comprised both DMPO- $\text{O}_2^{\cdot-}$ and DMPO- $\cdot\text{CH}_2\text{OH}$ adduct signals {spectra (c) and (d) of Figure 6} as witnessed by measurements of intensity and shape through the decay of ESR signals {spectra (g), (h), and (i) of Figure 6} in the dark because of differences in the half-lives of the different DMPO spin adducts. The adduct spectra varied from a complex series of signals to a simple $\cdot\text{CH}_2\text{OH}$ radical spectrum²⁰ on decay of the adduct with time. The signals for the DMPO- $\cdot\text{CH}_2\text{OH}$ adduct originate from attack of $\cdot\text{OH}$ radicals onto the CH₃OH solvent molecules by H abstraction after production of the $\cdot\text{OH}$ radical, consistent with the high reactivity of the $\cdot\text{OH}$ radical. More interestingly, addition of a small quantity of methanol to an aqueous TiO₂ dispersions displayed only DMPO- $\cdot\text{CH}_2\text{OH}$ adduct signals {spectrum (e) of Figure 6} rather than the expected DMPO- $\cdot\text{OH}$ adduct signals owing to the rapid reaction between $\cdot\text{OH}$ radicals and CH₃OH.

The above results leads to infer that the superoxide radical anion are produced first and remain stable in an organic solvent medium (at least in methanol). When the fraction of H₂O increases in the CH₃OH/H₂O mixed solvent system, the superoxide radical anion becomes unstable, especially in H₂O alone, being converted to an $\cdot\text{OH}$ radical; alternatively, the $\text{O}_2^{\cdot-}$ radical may accept another electron from TiO₂ particles, after electron injection from the excited dye SQ*, to yield the peroxide anion O_2^{2-} that in acid media forms H₂O₂, or the DMPO- $\text{O}_2^{\cdot-}$ may be converted into the DMPO- $\cdot\text{OH}$ adduct in aqueous media.²⁴

To assess further the possible involvement of either the superoxide radical anion or the DMPO- $\text{O}_2^{\cdot-}$ adduct in the generation of hydroxyl radicals, ESR experiments were carried out in aqueous TiO₂ dispersions containing the SQ dye (8.26 $\times 10^{-5}$ M) and the SOD enzyme which catalytically converts the superoxide radical anion to H₂O₂ and O₂. The intensity of the ESR signals of the DMPO- $\cdot\text{OH}$ adduct increases with increasing SOD concentration {spectra (b) and (c) of Figure 7}. In addition, to examine whether hydroxyl radical generation took place via reduction of H₂O₂, other experiments were performed under identical conditions in the presence of the H₂O₂ scavenging enzyme catalase in lieu of SOD. Addition of catalase diminished the intensity of the ESR signals attributable to DMPO- $\cdot\text{OH}$ adducts {spectra (d) and (e) of Figure 7}; these signals are barely discernible when 500 μL of catalase was added to the dispersion {spectrum (f)}. The results involving the enzymes SOD and catalase suggest that the $\cdot\text{OH}$ radical or the DMPO- $\cdot\text{OH}$ adduct originates from the reduction of H₂O₂ produced and not directly from $\text{O}_2^{\cdot-}$ or the DMPO- $\text{O}_2^{\cdot-}$ adduct, respectively. Such striking results persuasively confirm the correctness of eqs 3–5.

Proposed Pathway. Based on all the above direct evidence, the TiO₂-assisted degradation of the laser dye SQ under visible irradiation in aqueous dispersions takes place according to the process summarized by eqs 1–7. More details of the degradation process are demonstrated in Scheme 1. Excited dye SQ* first injects an electron to the conduction band of the TiO₂ particles; subsequently, the preadsorbed oxygen on the TiO₂ surface scavenges the electron to form the superoxide radical anion that can also accept another electron to yield O_2^{2-} ions which in acid media produce H₂O₂ (see Figure 5). To the extent that a larger quantity of H₂O₂ formed in the degraded solution, it is unlikely that the injected electrons were depleted for the formation of $\cdot\text{OH}$ radicals (eq 5) as ESR signals of the spin trapped $\cdot\text{OH}$ radical were observed. However, the possibility that the $\cdot\text{OH}$ radical attacks the SQ

dye molecule is not excluded because small quantities of other intermediates were also observed in the GC-MS experiments (see Figure 4) in addition to the principal intermediate product, the indolenium-2-one species. Decomposition of the dye begins with the dye's cation radical, SQ⁺, formed after electron injection, which then combines with oxygen rather than with the superoxide anion, subsequently undergoing decomposition of the organoperoxide radical cation through a complicated sequence of steps to ultimately yield the principal indolenium-2-one species, obtained principally by cleavage of the cyanine C=C double bond (see Figure 3). Evidently, there is selective oxidation of the C=C bond under the experimental conditions used, a process totally different from the pathway that implicates oxidation by $\cdot\text{OH}$ radicals produced by the UV light irradiation mechanism; the latter pathway usually results in the production of various small organic molecules and typically leads to total mineralization of the organic substrate to carbon dioxide, CO₂.

Acknowledgments

The authors appreciate the generous financial support of this work by the National Natural Science Foundation of China (No. 29677019, No. 29725715), the Foundation of the Chinese Academy of Sciences and the China National Committee for Science and Technology, and by a Grant-in-Aid for Scientific Research from the Ministry of Education (No. 066400757), Japan, and by the Natural Sciences and Engineering Research Council of Canada (No. A5443). We are also grateful to Prof. J. Chen for measurements of ESR spectra.

Literature Cited

- (1) Fox, M. A.; Dulay, M. T. *Chem. Rev.* **1993**, *93*, 341.
- (2) *Photocatalytic Purification and Treatment of Water and Air*; Ollis, D. F., Al-Ekabi, H., Eds.; Elsevier Science Publishers: Amsterdam, 1993.
- (3) Ollis, D. F.; Pelizzetti, E.; Serpone, N. *Environ. Sci. Technol.* **1991**, *25*, 1523.
- (4) Linsebigler, A. L.; Lu, G.; Yates, J. T., Jr. *Chem. Rev.* **1995**, *95*, 735.
- (5) (a) Hidaka, H.; Zhao, J.; Pellizzetti, E.; Serpone, N. *J. Phys. Chem.* **1992**, *96*, 2226. (b) Zhao, J.; Hidaka, H.; Takamura, A.; Pellizzetti, E.; Serpone, N. *Langmuir* **1993**, *9*, 1646.
- (6) Hidaka, H.; Asai, Y.; Zhao, J.; Pellizzetti, E.; Serpone, N. *J. Phys. Chem.* **1995**, *99*, 8244.
- (7) Rossetti, R.; Brus, L. E. *J. Am. Chem. Soc.* **1984**, *106*, 4336.
- (8) (a) Vinodgopal, K.; Kamat, P. V. *J. Photochem. Photobiol. A: Chem.* **1994**, *83*, 141. (b) Kamat, P. V.; Das, S.; Thomas, K. G.; George, M. V. *Chem. Phys. Lett.* **1991**, *178*, 75.
- (9) (a) He, J.; Zhao, J.; Shen, T.; Hidaka, H.; Serpone, N. *J. Phys. Chem.* **1997**, *101*, 9027. (b) Zang, L.; Qu, P.; Zhao, J.; Shen, T.; Hidaka, H. *Chem. Lett.* **1997**, 791. (c) Qu, P.; Zhao, J.; Shen, T.; Hidaka, H. *Colloids Surf. A* **1998**, *138*, 39.
- (10) (a) Vinodgopal, K.; Wynkoop, D.; Kamat, P. V. *Environ. Sci. Technol.* **1996**, *30*, 1660. (b) Nasr, C.; Vinodgopal, K.; Fisher, L.; Hotchandani, S.; Chattopadhyaya, A. K.; Kamat, P. V. *J. Phys. Chem.* **1996**, *100*, 8436.
- (11) Ross, H.; Bendig, J.; Hecht, S. *Solar Energy Mater. Solar Cells* **1994**, *33*, 475.
- (12) (a) Zhang, F.; Zhao, J.; Zang, L.; Shen, T.; Hidaka, H.; Pellizzetti, E.; Serpone, N. *J. Mol. Catal. A: Chem.* **1997**, *120*, 173. (b) Zhang, F.; Zhao, J.; Shen, T.; Hidaka, H.; Pellizzetti, E.; Serpone, N. *Appl. Catal. B: Environ.* **1998**, *15*, 147.
- (13) (a) Qu, P.; Zhao, J.; Shen, T.; Hidaka, H. *J. Mol. Catal. A: Chem.* **1998**, *129*, 257. (b) Zhao, J.; Wu, K.; Wu, T.; Hidaka, H.; Serpone, N. *J. Chem. Soc., Faraday Trans.* **1998**, *94*, 673.
- (14) (a) Wu, T.; Liu, G.; Zhao, J.; Hidaka, H.; Serpone, N. *J. Phys. Chem. B* **1998**, *102*, 5845. (b) Zhao, J.; Wu, T.; Wu, K.; Oikawa, K.; Hidaka, H.; Serpone, N. *Environ. Sci. Technol.* **1998**, *32*, 2394.
- (15) Lin, T.; Peng, B. *Dyes Pigments* **1997**, *35*, 331.
- (16) *Chinese National Standard: GB 11914-89* (1989).
- (17) Bader, H.; Sturzenegger, V.; Hoigne, J. *Water Res.* **1988**, *22*, 1109.

- (18) Walling, C. H. *Acc. Chem. Res.* **1975**, *8*, 125.
- (19) Barb, W. G.; Baxendale, J. H.; George, P.; Hargrave, K. R. *Trans. Faraday Soc.* **1951**, *47*, 591.
- (20) Makino, K.; Hagiwara, T.; Hagi, A.; Nishi, M.; Murakami, A. *Biochem. Biophys. Res. Comm.* **1990**, *172*, 1073.
- (21) Liu, Y.; Stolze, K.; Dadak, H.; Nohi, H. *Photochem. Photobiol.* **1997**, *66*, 443.
- (22) Zuo, Y.; Hoigne, J. *Science* **1993**, *260*, 71.
- (23) (a) Chance, B. *J. Biol. Chem.*, **1949**, *179*, 1341. (b) Jones, P.; Middlemiss, D. N. *Biochem. J.* **1972**, *130*, 411.
- (24) Halliwell, B.; J. M. C. Gutteridge, In *Free Radicals in Biology and Medicine*; Clarendon Press: Oxford, 1985; p 28.
- (25) Makino, K.; Hagiwara, T.; Imaishi, H.; Nishi, M.; Fujii, S.; Ohya, H.; Murakami, A. *Free Rad. Res. Comm.* **1990**, *9*, 233.

Received for review September 9, 1998. Revised manuscript received December 29, 1998. Accepted January 18, 1999.

ES980923I